

13

Long Gamma-Ray Burst Host Galaxies and their Environments

Johan P. U. Fynbo¹, Daniele Malesani¹, and Páll Jakobsson²

(1) *Dark Cosmology Centre, Niels Bohr Institute, The University of Copenhagen, Denmark*

(2) *Centre for Astrophysics and Cosmology, Science Institute, University of Iceland, Iceland*

13.1 Introduction

Host galaxies have played an important role in determining the nature of Gamma-Ray Burst (GRB) progenitors even before the first optical afterglows were detected. After the first detections of host galaxies, their properties provided strong evidence that long-duration GRBs were associated with massive stellar deaths and hence the concept of using long-duration GRBs to probe the evolution of the cosmic star-formation rate was conceived.

In this chapter we first briefly discuss some basic observational issues related to what a GRB host galaxy is (whether they are operationally well defined as a class) and sample completeness. We then describe some of the early studies of GRB hosts starting with statistical studies of upper limits done prior to the first detections, the first host detection after the *BeppoSAX* breakthrough and leading up to the current *Swift* era. Finally, we discuss the status of efforts to construct a more complete sample of GRBs based on *Swift* and end with an outlook. We only consider the host galaxies of long-duration GRBs. For short GRBs we refer to Berger (2009). The study of GRB host galaxies has previously been reviewed by van Paradijs et al. (2000) and Djorgovski et al. (2003).

13.2 Early results based on GRB host galaxy studies

13.2.1 Pre-afterglow host galaxy studies

Prior to the first afterglow detections a few gamma-ray bursts with relatively small uncertainties on their derived position were studied based on the Interplanetary Network (Hurley et al. 1993; see also Chapter 2). Limits on host galaxy magnitudes in such boxes coupled with distance estimates based on $\log N$ vs. $\log S$ arguments (see also Chapter 3) suggested that GRB

host galaxies predominantly had to be subluminal (Fenimore et al. 1993). However, such limits depended strongly on the assumed GRB luminosity function. As argued by Woods & Loeb (1995), above a certain width of the GRB luminosity function the probability of detection of the then possibly very distant GRBs with apparently faint hosts would be considerable (see also Larson 1997 and Wijers et al. 1998). In fact both explanations turned out to contain part of the truth.

13.2.2 The first host galaxy detections

Obviously, the detection of the first optical afterglows (van Paradijs et al. 1997) fundamentally changed the study of host galaxies. The first detection of an extended source at the position of a GRB afterglow was for GRB 970228 (Sahu et al. 1997) – the first GRB with a detected X-ray and optical afterglow (Costa et al. 1997, van Paradijs et al. 1997). At the time, it was not firmly proven that this extended source actually was the host galaxy so the distance scale of GRBs was yet to be established. The next GRB with a detected optical afterglow was GRB 970508. This burst was found to have a redshift of 0.695 (Metzger et al. 1997) and hence the extragalactic nature of (the majority of) long-duration GRBs was established. GRB hosts were subsequently soon found to be predominantly blue, star-forming galaxies, suggesting a young population origin for the bursts (Paczynski 1998, Hogg et al. 1999, Christensen et al. 2004). Another important point was clear after the detection of GRB 970508, namely that GRBs allow the detection of distant (star-forming) dwarf galaxies that are very difficult to detect with other methods (Natarajan et al. 1997).

A few months later relatively deep, early limits were obtained on the magnitude of the optical afterglow of GRB 970828. The non-detection of this optical afterglow suggested that some GRBs occur along sightlines with substantial dust extinction in the observed optical band (Groot et al. 1998). The third[†] GRB to have its optical afterglow detected was GRB 971214 for which a redshift of $z = 3.42$ was established from the likely host galaxy (Kulkarni et al. 1998). Hence, it was immediately clear that GRBs allow us to probe ongoing star-formation throughout the observable Universe (e.g., Wijers et al. 1998).

In late March 1998 two further optical afterglows were detected and then in April, GRB 980425 was found to be associated with a hyperluminous type Ic SN in a nearby dwarf galaxy at redshift $z = 0.0085$ (Galama et al.

[†] Much later, in 2003, it was established that an optical afterglow was also detected for GRB 970815 (Soderberg et al. 2004).

1998). The intrinsic fluence of this burst was about 4 orders of magnitude fainter than the GRBs with optical afterglows studied before and hence this discovery started discussions both on low-luminosity bursts and the issue of chance projection. It is remarkable that roughly within a year after the first detected optical afterglow some of the most important conclusions were already reached: GRBs are related to massive stellar deaths, are located predominantly in star-forming dwarf galaxies, are detected throughout most of the observable Universe, are sometimes hidden by dust, and there seems to be a population of low-luminosity GRBs only detectable in the relatively local Universe.

13.3 Operational issues related to GRB host galaxy studies

After having established that (at least the majority of) GRBs have hosts we make a short interlude discussing operational issues related to GRB host galaxies as a class. It is prudent to keep these points in mind whenever considering conclusions made about GRB hosts and their relation to other classes of in particular high-redshift galaxies.

13.3.1 Dark bursts and incomplete samples

A crucial issue when discussing the nature of GRB host galaxies and the implication thereof on the nature of GRB progenitors is sample completeness. The detection of the GRB itself is of course limited by the sensitivity of the gamma-ray detector and the GRB sample from a given mission will hence be representative of a smaller and smaller part of the (possibly evolving) GRB fluence distribution as one moves to higher and higher redshifts. However, in terms of observational selection bias, the GRB detection should not be affected by host galaxy properties. In contrast, detection of the longer wavelength afterglow emission, which is crucial for obtaining the precise localization as well as measuring redshifts (see, e.g., Fiore et al. 2007), is strongly dependent on the dust column density along the line-of-sight in the host galaxy.

In the samples of GRBs detected with satellites prior to the currently operating *Swift* satellite the fraction of GRBs with detected optical afterglows was only about 30% (Fynbo et al. 2001, Lazzati et al. 2002). Much of this incompleteness was caused by random factors affecting ground-based optical observations, such as weather or unfortunate celestial positions of the bursts, but some remained undetected despite both early and deep observations. It is possible that some of these so called “dark bursts” could be

caused by GRBs in very dusty environments (Groot et al. 1998) and hence the sample of GRBs with detected optical afterglows could very well be systematically biased against dust obscured hosts (see also Jakobsson et al. 2004a, Rol et al. 2005, 2007, Jaunsen et al. 2008, Tanvir et al. 2008 for more recent discussions of the dark bursts). Other causes for having a very faint optical afterglow are high redshifts (e.g. Greiner et al. 2009, Ruiz-Velasco et al. 2007) or – but only to some extent – intrinsically hard spectra (e.g., Pedersen et al. 2006). In any case, such a high incompleteness imposes a large uncertainty on statistical studies based on GRB host galaxies derived from these early missions.

It should be stressed that the conclusions based on these samples may only be relevant for a minority of all GRBs and consequently a biased subsample of the GRB host population. Galaxies hosting GRBs located in high-metallicity and hence more dusty environments, (and we know already that such systems exist), will be systematically underrepresented. Due to the much more precise and rapid X-ray localization capability of *Swift* it is possible to build a much more complete sample of GRBs from this mission as we will discuss later in this chapter.

13.3.2 Contamination from chance projection and Galactic transients

An important question to ask is: are GRB host galaxies operationally well-defined as a class? The answer may seem to be trivially “yes”, but reality is more complex. If we define the host galaxy of a particular burst to be the galaxy nearest to the line-of-sight, we need to worry about chance projection (Sahu et al. 1997, Band & Hartmann 1998, Campisi & Li 2008, Cobb & Baylin 2008). In the majority of cases where an optical afterglow has been detected and localized with subarcsecond accuracy and where the field has been observed to deep limits, a galaxy has been detected with an impact parameter less than 1 arcsec (see, e.g., Bloom et al. 2002, Fruchter et al. 2006 and Fig. 13.1 for an example). The probability for this to happen by chance depends on the magnitude (and angular size) of the galaxy. The number of galaxies per arcmin² has been well determined to deep limits in the various Hubble deep fields. To limits of $R = 24$, 26 and 28 there are about 20, 80 and 400 galaxies arcmin⁻². Hence, the probability to find an $R = 24$ galaxy by chance in an error circle with radius 0.5 arcsec is about 4×10^{-3} . For an $R = 28$ galaxy the probability is about 8%. If the error circle is defined only by the X-ray afterglow (with a radius of 2 arcsec in the best cases) then we expect a random $R = 24$ and $R = 28$ galaxy in 6% and all

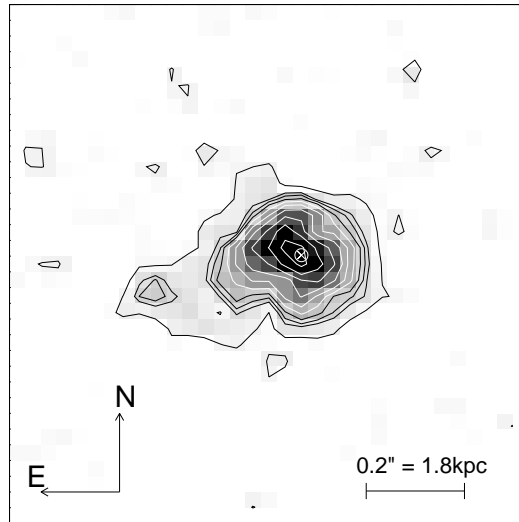


Fig. 13.1. The *HST* 1×1 arcsec² field around the host galaxy of GRB 021004 at $z = 2.33$ found with *HETE-2* (from Fynbo et al. 2005). The GRB went off near the center of the galaxy. The position of the GRB is marked with a cross and an error circle and in coincides with the centroid of the galaxy to within a few hundredths of an arcsec. In cases like this there is no problem in identifying the correct host galaxy. However, in cases of bursts localized to only a few arcsec accuracy, chance projection needs to be considered.

of the error circles. For a sample of a few hundred GRBs chance projection should hence not be a serious concern for GRBs localized to subarcsecond precision, but for error-circles with radius of a few arcseconds we expect many chance projections. In some cases it may be possible to eliminate the chance projections, e.g., based on conflicting redshift information from the afterglow and proposed host (e.g., Jakobsson et al. 2004b); without such extra information this is impossible.

Finally, it is worth noting that some events triggering the gamma-ray detectors are Galactic high-energy transients rather than extragalactic GRBs. Examples are GRB 070610 (Kasliwal et al. 2008, Castro-Tirado et al. 2008) later renamed to SWIFT J195509.6+261406 and GRB 060602B, which was found to be a low-mass X-ray binary (Wijnands et al. 2009). Judged from the high energy properties alone these bursts looked just like GRBs, so in principle such events can contaminate GRB samples. Presumably, most of these events will, like these two examples, be located at low Galactic latitude and hence most can be rejected based on a Galactic latitude cut in the sample selection.

13.4 Status prior to the *Swift* mission

13.4.1 GRBs as probes of star formation

As outlined above, the properties of the first handful of detected hosts showed a clear link to star-formation. Moreover, Mao & Mo (1998) made a model incorporating a power-law shaped luminosity function of GRBs and the assumption that the GRB rate is proportional to the cosmic star-formation density. From this model, Mao & Mo (1998) were able to get remarkably good agreement with the properties of observed hosts suggesting that GRBs were close to being good tracers of star-formation. Hogg & Fruchter (1999) reached a similar conclusion.

13.4.2 Biased tracers?

However, as the sample size grew evidence started to collect suggesting that GRBs may be related only to massive stars with metallicity below a certain threshold. As discussed in Chapter 10, such a metallicity dependence is expected in the collapsar model. The first empirical evidence for this came with the realization that the GRB hosts were fainter and bluer than expected according to certain models about the nature of the galaxies dominating the integrated (over all galaxies) star-formation rate density (Le Floc'h et al. 2003, see also Fig. 13.2). Also, SCUBA imaging of GRB hosts in the sub-mm range produced only a few rather tentative detections, again seemingly at odds with the expectations if GRB hosts were selected in an unbiased way from all star-forming galaxies (Tanvir et al. 2004). The analysis is complicated, and it has been pointed out by Priddey et al. (2006) that “there is sufficient uncertainty in models and underlying assumptions, as yet poorly constrained by observation (e.g., the adopted dust temperature) that a correlation between massive, dust-enshrouded star formation and GRB production cannot be firmly ruled out.” The issue of dust temperature has been discussed in detail by Michałowski et al. (2008; see also Fig. 13.3). They find that the few GRB hosts that have been tentatively detected in the sub-mm range have hotter dust and lower masses than typical sub-mm detected galaxies.

Further circumstantial evidence for a preference towards low metallicity came from the observation that Lyman- α ($\text{Ly}\alpha$) emission seemed to be ubiquitous from GRBs hosts (Fynbo et al. 2003a, Jakobsson et al. 2005b). At this point, around 2003, redshifts had been measured for ten $z > 2$ GRBs. $\text{Ly}\alpha$ emission was detected for 5 of these and for the remaining 5 it was not yet searched for to sufficient depth to allow detection of even a large equiv-

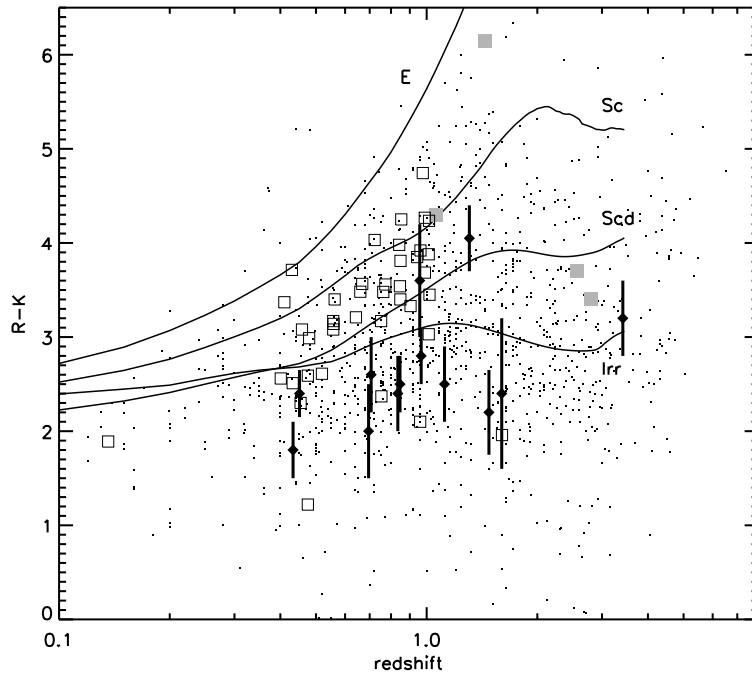


Fig. 13.2. Observed $R - K$ colours versus redshift for the sample of GRB host galaxies selected by Le Floch et al. (2003) (*filled diamonds*). The point of the figure is that GRB host galaxies are bluer than other starburst galaxies studied at similar redshifts. For comparison the authors also plot the colours and redshifts for optically-selected field sources (*dots*) and of ISO sources from the Hubble Deep Field (*open squares*) and of SCUBA galaxies with confirmed redshifts (*filled squares*). See Le Floch et al. (2003) for more details and references. In addition, the authors found that the K -band luminosities of GRB hosts were substantially fainter than, e.g., the ISO galaxies which at redshifts around one are believed to dominate the total star-formation activity. Solid curves indicate the observed colours of local E, Sc, Scd and Irr galaxies if they were moved back to increasing redshifts.

alent width emission line. As only 25% of continuum selected starbursts at similar redshifts are $\text{Ly}\alpha$ emitters and as $\text{Ly}\alpha$ emission on theoretical grounds should be more common for metal poor starbursts (Charlot & Fall 1993; but see also Mas-Hesse et al. 2003) this suggested that there could be a low metallicity bias in making GRBs. However, the reason could also be an observational bias against dusty (and hence likely higher metallicity) GRBs or simply that the majority of the star formation is associated with low-luminosity galaxies, which tend to be metal poor in accordance with the luminosity-metallicity relation. The broad-band luminosity distribution of $z > 2$ GRB hosts was found by Jakobsson et al. (2005b) to be consistent with the assumption that GRBs are selected from the rest-frame UV selec-

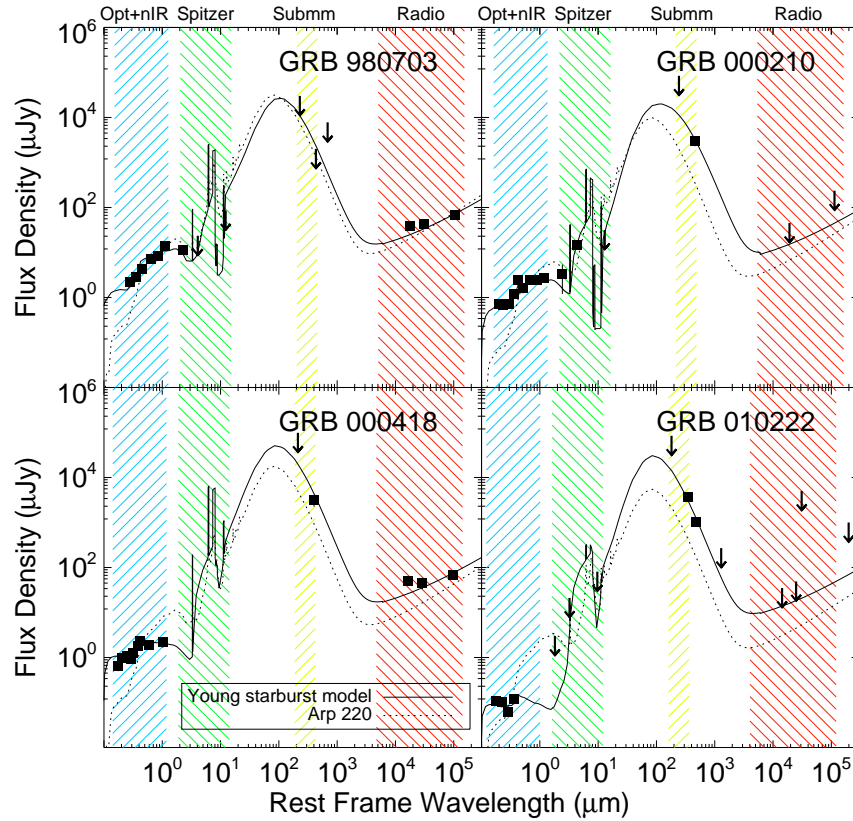


Fig. 13.3. Broad-band spectral energy distribution of four GRB hosts with firm submillimetric or radio detections, demonstrating the role played by observations in various wavebands (from Michałowski et al. 2008). Dotted lines show the rescaled SED of the prototypical ultraluminous infrared galaxy Arp 220, while solid lines show synthetic best-fit models based on the GRASIL code (Silva et al. 1998).

tion function based on the total UV emission per luminosity bin. Assuming that the rest-frame UV emission is proportional to the star formation rate this suggested that GRBs cannot be strongly biased towards low metallicity.

A very important result is that GRBs and core-collapse (CC) SNe are found in different environments (Fruchter et al. 2006 and Fig. 13.4). GRBs are significantly more concentrated on the very brightest regions of their host galaxies than CC SNe. The same study also found that GRB host galaxies at $z < 1$ are fainter and more irregular than the host galaxies of CC SNe. Fruchter et al. (2006) suggest that these results may imply that

long-duration GRBs are associated with the most extremely massive stars and may be restricted to galaxies of limited chemical evolution. This would directly imply that long-duration GRBs are relatively rare in galaxies such as our own Milky Way.

This study is also based on incomplete pre-*Swift* samples, but as the SN samples are, if anything, more biased against dusty regions than GRBs, the fact that GRB hosts have lower luminosities than CC SN hosts does seem to provide substantial evidence that GRBs are biased towards massive stars with relatively low metallicity. Regarding the size of the effect, Wolf & Podsiadlowski (2007) find, based on an analysis of the Fruchter et al. (2006) data, that the metallicity threshold cannot be significantly below half the solar metallicity. Concerning the different environments of CC SNe and GRBs it has recently been found that type Ic SNe have similar positions relative to their host galaxy light profiles as GRBs, whereas all other SN types have (similar) distributions less centred on their host light than GRBs and SN Ic (Kelly et al. 2007).

Larsson et al. (2007), modeling the distribution of young star clusters and total light in the local starburst NGC 4038/39 (the Antennae), find that the different distributions of GRBs and CC SNe relative to their host light can be naturally explained by assuming different mass ranges for the typical progenitor stars: $> 8 M_{\odot}$ for typical CC SNe and $> 20 M_{\odot}$ for GRB progenitors. The picture is complicated by the finding that type Ic SNe typically are found in substantially more metal rich environments than GRBs (Modjaz et al. 2008). It is well established that WR stars become more frequent with *increasing* metallicity - opposite to GRBs that, if anything, are biased towards low metallicity. Taken together, these results suggest that progenitors of GRBs and “normal” type Ic SNe are two different subsets of the $> 20 M_{\odot}$ stars. For a thorough discussion of the relation between WR stars, SN Ic and GRBs we refer to Crowther (2007). In conclusion, there seems to be a low metallicity preference for GRBs, but the metallicity threshold cannot be much below half solar and we need a more unbiased and uniform sample to estimate the severity of the effect (see also Chapter 10).

13.4.3 The galactic environment of GRB hosts

The galactic environments of GRBs have so far not been studied much. At low redshifts Foley et al. (2006) studied the field of the GRB 980425 host galaxy, which was reported to be a member of a group. However, based on redshift measurements of the proposed group members, Foley et al. (2006)

could establish that the host of GRB 980425 is an isolated dwarf galaxy[†]. Levan et al. (2006) also proposed GRB 030115 to be connected to a cluster around $z \sim 2.5$ based on photometric redshifts. At redshifts $z \gtrsim 2$ a few GRB fields have been studied using narrow band Ly α imaging (Fynbo et al. 2002, Fynbo et al. 2003a, Jakobsson et al. 2005b). In all cases several other galaxies at the same redshift as the GRB host were identified, but it is not certain whether the galaxy densities in these fields are higher than in blank fields as no blank field studies have been carried out at similar redshifts. However, the density of Ly α emitters was found to be as high as in the fields around powerful radio sources that have been proposed to be forming proto-clusters (Kurk et al. 2000), which would suggest that GRBs could reside in overdense fields at $z \gtrsim 2$. Bornancini et al. (2004), on the other hand, argue for a low galaxy density in GRB host galaxy environments. In conclusion, the evidence is currently too sparse to establish whether GRB hosts are located in special environments.

13.4.4 GRB host absorption line studies

GRB host galaxies have the unique advantage over galaxies selected on the base of their emission that spectroscopy of their afterglows (X-ray, optical, and other bands) can reveal detailed information about the gas in the host galaxy ranging from the circumstellar material to halo gas.

Two interesting examples of what GRB afterglow spectroscopy can teach us about GRB hosts are the cases of GRB 030323 at redshift $z = 3.372$ (Vreeswijk et al. 2004) and GRB 080607 at $z = 3.036$ (Prochaska et al. 2009). As seen in Fig. 13.4 the host galaxy of GRB 030323 is among the faintest detected (it has a magnitude of about $R = 28$). The spectrum of the optical afterglow of the event is shown in Fig. 13.6. The dominant feature in the spectrum is a very large damped Ly α absorption (DLA) line corresponding to a redshift of $z = 3.37$ (shown in more detail in the inset in the upper left corner). A DLA is a hydrogen absorption line with column density above $2 \times 10^{20} \text{ cm}^{-2}$, where the total equivalent width is dominated by the broad damping wings. Also seen are numerous low- and high-ionization lines at a redshift $z = 3.3718 \pm 0.0005$. The inferred neutral hydrogen column density, $\log(N_{\text{HI}}/\text{cm}^{-2}) = 21.90 \pm 0.07$, is very large – higher than in DLAs seen against the light of QSOs (Wolfe et al. 2005). From an analysis of the metal line strengths compared to the hydrogen column density, a sulphur abundance of about 0.05 solar is determined. An upper limit to the H₂

[†] H α imaging of the host has revealed a very faint companion about 1 arcmin NE of the host (L. Christensen, private communication).

molecular fraction of $2N_{\text{H}_2}/(2N_{\text{H}_2} + N_{\text{HI}}) < 10^{-6}$ is derived from an analysis of the absence of molecular lines.

In the DLA trough, a Ly α emission line is detected, which corresponds to a star formation rate (not corrected for dust extinction) of roughly $1 M_{\odot} \text{ yr}^{-1}$. All these results are consistent with the host galaxy of GRB 030323 containing low metallicity gas with a low dust content. In addition, fine-structure lines of silicon, Si II*, are detected in the spectrum. These have not been clearly detected in QSO-DLAs suggesting that these lines are produced in the vicinity of the GRB explosion site. The optical spectrum of GRB 080607 displays an even larger HI column density of $\log(N_{\text{HI}}/\text{cm}^{-2}) = 22.7$, but contrary to GRB 030323, the GRB 080607 host is responsible for a very metal rich absorption system (close to solar metallicity) with significant dust extinction and a clear detection of both H₂ and CO molecular absorption (Fig. 13.7). At the time of writing (June 2010) the host galaxy has not been detected.

Dozens of similar quality spectra have been obtained, some with high resolution spectrographs (e.g., Chen et al. 2005, Starling et al. 2005, Vreeswijk et al. 2007, D’Elia et al. 2007). The properties of the GRB absorbers as a class are discussed in Savaglio (2006), Fynbo et al. (2006) and Prochaska et al. (2007). The GRB absorbers are characterized by HI column densities spanning five orders of magnitude from $\sim 10^{17} \text{ cm}^{-2}$ to $\sim 10^{23} \text{ cm}^{-2}$ and metallicities spanning two orders of magnitude from 1/100 to nearly solar (see Fig. 13.5). Calura et al. (2009) have taken the first steps towards modelling the abundance ratios in GRB hosts using models for chemical evolution in galaxies. The majority of the GRB absorbers have metallicities exceeding the cosmic mean metallicity of atomic gas at $z > 2$ as determined from QSO-DLAs. The difference in abundances between the QSO DLAs and GRB absorbers can be reconciled in a simple model where the two populations are drawn randomly from the distribution of star-forming galaxies according to their star formation rate and HI cross section, respectively (Fynbo et al. 2008). However, it should be noted that these results are based on a small sample of GRBs in which most have bright optical afterglows.

13.5 GRB host galaxies in the *Swift* era

The currently operating *Swift* satellite (Gehrels et al. 2004 and Chapter 5) has revolutionized GRB research with its frequent, rapid, and precise localization of both long and short duration GRBs. The breakthrough enabled by *Swift* was the ability to build a much more complete sample of localized

GRBs and hence of GRB host galaxies. By complete we here mean unbiased in terms of the optical properties of the GRB afterglows.

13.5.1 Building a complete sample of *Swift* GRBs

The *Swift* satellite has been superior to previous GRB missions due to the combination of several factors: *i*) it detects GRBs at a rate of about two bursts per week, about an order of magnitude larger than the previous successful *BeppoSAX* and *HETE-2* missions; *ii*) with its X-Ray Telescope (XRT) it localizes the bursts with a precision of about 5 arcsec (often later refined to less than 2 arcsec), also orders of magnitude better than previous missions; *iii*) it has a much shorter reaction time, allowing the study of the evolution of the afterglows literally seconds after the burst, sometimes while the prompt γ -ray emission is still being emitted. For a detailed description of the *Swift* era see also Chapter 5.

We will here discuss the status of an ongoing effort to build such a complete sample (see, e.g., Jakobsson et al. 2006a for earlier descriptions of this work). Rather than including all *Swift* detected GRBs only those GRB afterglows with favourable observing conditions are included, in particular those fulfilling the following selection criteria:

- (i) XRT afterglow detected within 12 hr;
- (ii) small foreground Galactic extinction: $A_V < 0.5$ mag;
- (iii) favourable declination: $-70^\circ < \delta < +70^\circ$;
- (iv) Sun-to-field angular distance larger than 55° .

By introducing these constraints the sample is not biased towards GRBs with optically bright afterglows, but will contain bursts for which useful follow-up observations are likely to be secured.

The fact that 6–10 m class telescopes have made tremendous efforts to secure redshifts means that this sample has a much higher redshift completion than for pre-*Swift* samples (see Fig. 13.8). Still, it is clear that we will not get redshifts for all bursts from spectroscopy of the afterglows for multiple reasons. In a small fraction of the cases where a spectrum of the afterglow is secured no redshift can be measured. This is either due to lack of significantly detected absorption lines or because the spectrum is simply too noisy. For these bursts the only way to measure the redshift is via spectroscopy of the host galaxy, but this is a challenging task due to the faintness of most GRB hosts (see below).

13.5.2 The redshift distribution of Swift GRBs: current status

The first conclusion from Fig. 13.8 is that most *Swift* GRBs are very distant. *Swift* GRBs are more distant than GRBs from previous missions due to the higher sensitivity of the satellite to the lower energies prevalent in the more distant events (Fiore et al. 2007). The faster reaction time of the satellite probably also contributes to shifting the median redshift upwards. The median and mean redshift are now both around 2, while for previous missions it was closer to 1 (Jakobsson et al. 2006a). The record holders are GRB 080913 at $z = 6.7$ (Greiner et al. 2009; Pattel et al. 2010) and GRB 090423 at $z = 8.2$ (Tanvir et al. 2010; Salvaterra et al. 2010). It is striking how events at redshifts as large as ~ 8 can be detected within such a small sample. For comparison, only a few QSOs are detected at $z \sim 6$ (and none at $z \sim 8!$) out of a sample of hundred thousand QSOs. Given the current redshift completeness level, the data are consistent with a broad range of redshift distributions (see, e.g., Jakobsson et al. 2006a).

13.5.3 HI column densities

The HI column density distribution for GRB sightlines is extremely broad. It covers a range of about 5 orders of magnitude from $\sim 10^{17} \text{ cm}^{-2}$ (Fig. 13.9, Chen et al. 2007) to nearly 10^{23} cm^{-2} (Jakobsson et al. 2006b). It still remains to be understood if this distribution is representative of the intrinsic distribution of HI column densities towards massive stars in galaxies or if the distribution is rather controlled by the ionizing emission from the afterglows themselves. In any case, as pointed out by Chen et al. (2007), the HI column density distribution provides an upper limit to the escape fraction of Lyman continuum emission from star-forming galaxies. This is crucial for the issue of determining the sources for the ionising photons in the metagalactic UV background.

13.5.4 Extinction

In addition to HI column densities, metal and molecular abundances and kinematics, the afterglow spectra also provide information about the extinction curves. The intrinsic spectrum of the afterglow is predicted from theory to be a power-law and therefore any curvature or other broad features in the spectrum can be interpreted as being due to the extinction curve shape. So far, almost all the extinction curves derived for GRB sightlines have been consistent with an extinction curve similar to that of the SMC (e.g., Starling et al. 2007, Schady et al. 2010). Recently, a clear detection of the 2175 Å

bump known from the Milky Way was found in a $z = 2.45$ GRB sightline (Elíasdóttir et al. 2009, Krühler et al. 2008 and Fig. 13.10). This GRB absorber also has unusually strong metal lines suggesting that the presence of the 2175 Å extinction bump is related to high metallicity (as expected from sightlines in the local group). However, we have examples of GRBs with nearly solar metallicity for which the bump is not seen, so it seems that metallicity is not the only parameter controlling the presence of the 2175 Å extinction bump. Concerning the amount of extinction, the GRB sightlines vary from no extinction (e.g., GRB 050908, Fig. 13.9) to $A_V > 5$ mag (e.g., GRB 070306, Jaunsen et al. 2008).

13.5.5 The host sample

Hjorth and collaborators have been working on building up a sample of *Swift* GRB host galaxies observed with the ESO *VLT*. The main science driver for this work is to build a representative, unbiased sample of GRB host galaxies that can be used to firmly establish the statistical properties of GRB hosts. Similar to the philosophy of the afterglow sample discussed above, this work focusses on the systems with the best observability, which also have the best available information. GRBs included in the sample fulfil the following criteria:

- (i) triggered by BAT;
- (ii) belong to the long-duration class;
- (iii) trigger time between March 2005 and August 2007;
- (iv) low Galactic extinction ($A_V \leq 0.5$ mag);
- (v) prompt XRT localization (< 12 hr);
- (vi) good observability from the *VLT* ($-70^\circ < \delta < +27^\circ$);
- (vii) small position error (radius $\leq 2''$) from based on the X-ray afterglow astrometry.

Note that criteria (iii)–(vi) do not introduce selection effects in the sample, since they are not based on intrinsic properties of the GRBs. Only criterion (vii) may in principle bias against faint events (which will have on the average worse localizations), however in practice it only excludes a few events (3% of the total). On the other hand, a burst satisfying all the above criteria must have been on the average better studied and characterized, since its afterglow was well observable from the ground.

There are 69 GRBs fulfilling the above criteria. For 52 (75%) of these the optical/NIR afterglow has been detected and for 38 (55%) the redshift has been measured (spanning the range $0.033 < z < 6.295$). Figure 13.11

shows the distribution of this sample in the sky. For more details about the program, we refer to Hjorth et al. (2012).

13.5.5.1 Results

Magnitudes. The primary objective in this study is the search and localization of the hosts. The applied strategy is a moderately deep R -band exposure (30 min), followed by deeper imaging (~ 2 hr) in case of no detection. The survey was quite successful, with a detection rate of 80% of the hosts. The success rate drops significantly at large redshifts, with a recovery fraction of 40% for GRBs with a measured redshift larger than 3. Figure 13.12 shows the distribution of the observed and absolute magnitudes. To compute the k -corrections, a spectrum $F_\nu \propto \nu^{-1}$ was assumed. As can be seen, most GRB hosts are subluminal, at a level $(0.01-1) \times L^*$. This is in line with the previous findings mentioned above based on smaller and less complete samples (Le Floch et al. 2003, Fruchter et al. 2006). Hence, this conclusion is not a result of a bias against dusty GRB hosts, but it is an intrinsic property of the GRB host population.

Colours. In addition to R -band imaging the Hjorth et al. (2012) survey also obtained K -band imaging of all the fields. The detection rate at NIR wavelengths is significantly lower than in the optical. Hosts were detected in only about 40% of the systems in the sample. Overall, colours are in the range $2 < R - K < 4.5$, with two possible examples of extremely red objects (EROs) with $R - K \approx 5$. These GRBs had no reported optical afterglow. While the lack of optical emission is consistent with the presence of dust (and reddening), a chance association between the GRB and the galaxy cannot be excluded. Figure 13.13 shows the distribution of observed colours for bursts with and without an optical afterglow. Note that the two groups have a comparable distribution of colours. Overall, even considering bursts with no detected optical afterglow, the earlier findings of Le Floch et al. (2003) that GRB hosts have mostly blue colours are confirmed (though a few cases of red systems have been found (Levan et al. 2006, Berger et al. 2007). This does not exclude that dust is present in these objects (e.g. Jaunsen et al. 2008, Tanvir et al. 2008), but is probably confined only in a fraction of the volume occupied by the young stars (Michałowski et al. 2008).

Redshifts. Hosts without known redshift were observed with a variety of spectroscopic setups (Jakobsson et al. 2012, Krühler et al. 2012). In several cases, only upper and/or lower limits could be placed on the redshift due to the lack of prominent features. Many GRBs are bound to be in the so-called redshift desert ($1 \lesssim z \lesssim 2$), where the most prominent nebular lines

are shifted into wavelength regions difficult to observe. In some cases, this hypothesis was confirmed thanks to the use of red grisms sensitive up to 10,000 Å, which probes redshifts up to $z \approx 1.7$ through the [O II] emission line.

Overall, 15 new redshifts were determined from host galaxy spectroscopy, and, surprisingly, a few of the redshifts reported in the literature were found to be inconsistent with the redshift derived from the likely host. This is most likely not due to a wrong host identification as these are bursts with detected optical afterglows (and for some the reported wrong redshifts were based on emission lines). For an additional three systems the redshift could be constrained in the range $1 \lesssim z \lesssim 2$. Surprisingly, only three of the targeted systems have a redshift larger than 2. While this is partly due to the selection of the brightest systems for spectroscopy, it also shows that many dark or optically faint GRBs probably lie at moderate redshifts. Fig. 13.14 shows the redshift distribution of the sample, outlining the contribution from the Hjorth et al. (2012) program. We caution that the analysis of the spectroscopic data is not yet complete. The most noticeable effect is the reduction of the “gap” at $z \sim 1.7$, which was likely due to the lack of prominent features in the observed spectral range, for both GRB afterglows and hosts (Fiore et al. 2007).

Ly α emission. For all hosts with a known redshift in the range $2 < z < 4.5$ (where the Ly α falls in a favorable wavelength range), a spectrum was obtained with the aim of looking for Ly α in emission (Milvang-Jensen et al. 2012). The presence of a host galaxy detection in the optical was not required as Ly α can easily be detected from galaxies that are very faint in the continuum (e.g., Fynbo et al. 2003b). These spectra also provided a way to double check some of the redshifts reported in the literature (leading to the aforementioned discovery of a few likely wrong redshifts). The recovery fraction for these *Swift* GRB hosts is lower than in earlier cases (with moderately deep exposures of 1.5–4 hr). Ly α is detected in about 35% of the cases. As mentioned above, pre-*Swift* studies provided five detections out of five studied cases (Fynbo et al. 2003a). The peak of the Ly α line is observed to be redshifted by a few hundred km s $^{-1}$ with respect to the absorption-line redshift inferred from afterglow spectroscopy. This has been already observed in Lyman break galaxies (e.g., Adelberger et al. 2003).

In summary, the Hjorth et al. (2012) study of *Swift* hosts has established that many of the conclusions reached from the smaller and more biased pre-*Swift* samples still hold: GRB hosts are all star forming and they are predominantly (but not all) subluminal and blue.

13.6 Simulations of GRB host galaxies

In this final section we will briefly discuss the work that has been done on simulating and modeling GRB host galaxies. The modeling of star-forming galaxies in their cosmological context is a field in rapid progress. Whereas the treatment of growth of structure in the dark matter component seems to be very well understood it is still far from trivial to include the baryonic physics. In particular star formation and its feedback on the interstellar medium are difficult to include in the simulations. Different “recipes” exist, but it is difficult objectively to establish if they provide an adequate description of reality rather than providing, e.g., a fitting parameter that helps reproducing a set of observations. GRB host galaxies are interesting for testing simulations of galaxies due to their nature as star-formation selected galaxies. Hence, it is relatively easy to predict from a given simulation what the properties (e.g., luminosities, metallicities, environments, etc.) of a sample of GRB host galaxies should be under the assumptions behind the simulation. This work has only started recently and there is certainly potential for a lot of development in this area. The first pioneering work was done by Courty et al. (2004, 2007) who basically established that galaxies similar to the GRB hosts exist in their simulations. Nuza et al. (2007) predicted the properties of GRB hosts under the assumption that GRBs are only formed by low-metallicity stars. The study used a rather small simulated volume with a box length of only 10 Mpc, but it was still an important step forward. Most lately, Nagamine et al. (2008) used a similar simulation to examine the HI absorption of GRB host absorption systems as a function of redshift.

13.7 Conclusions and outlook

About a decade after the first detection of host galaxies we have progressed tremendously. GRBs host galaxies have been found to be predominantly young, actively star-forming and subluminal. This conclusion seems to reflect the intrinsic properties of the host populations and is not only a result of selection effects. The study of the GRB host absorption systems is an entire new emerging field providing an interesting link between the study of QSO-DLAs and star-forming galaxies selected in emission.

There are still unclarified issues. One of the most important questions to answer is whether GRBs trace all star-formation or only a limited, low-metallicity segment. The evidence seems to point in different directions. Most likely the road to further progress will be by building yet more complete samples with more detailed information for all GRBs and their hosts (metallicities, luminosities, dust masses, etc.). Bursts like GRB 080607 (Prochaska

et al. 2009) and GRB 070306 (Jaunsen et al. 2008) suggest that we do preferentially lose GRBs in high metallicity, dusty environments. We need to establish the frequency of such systems in the host population to determine where GRBs fit into the big picture. Also, more work is needed on improving the predictions of how the properties of GRB hosts should be under various assumptions about the link between GRBs and star-formation.

Another important area for future work is the use of GRBs to probe galaxies at the epoch of re-ionization. It is now established that GRBs allow us to move further back in time than what is currently possible with QSOs (Greiner et al. 2009, Tanvir et al. 2010, Salvaterra et al. 2010). The discovery of bursts like GRB 090423 also allows us to study in what type of galaxies most of the star formation happened at $z > 8$, and what was the nature of the sources responsible for the re-ionization. There is evidence that the bright $z > 6$ galaxies discovered using colour-colour (drop-out) selection or more advanced photometric redshifts are too rare to provide the total star formation rate as well as to have done the re-ionization (e.g., Bouwens et al. 2007). GRB measurements provide the tool to find the more typical galaxies responsible for the bulk of the production of ionizing photons (Ruiz-Velasco et al. 2007), and will allow further study of these galaxies in the future (e.g., with *JWST* or 30m ground-based telescopes).

References

- Adelberger, K.L., et al. (2003). *ApJ* **584**, 45.
 Band, D. L., & Hartmann, D. H. (1998). *ApJ* **493**, 555.
 Berger, E., et al. (2007). *ApJ* **660**, 504.
 Berger, E. (2009). *ApJ* **690**, 231.
 Bloom, J. S., Kulkarni, S. R., & Djorgovski, S. G. (2002). *AJ* **123**, 1111.
 Bornancini, C. G., et al. (2004). *ApJ* **614**, 84.
 Bouwens, R. J., et al. (2007). *ApJ* **670**, 928.
 Calura, F., et al. (2009). *ApJ* **693**, 1236.
 Campisi, M. A. & Li, L.-X. (2008). *MNRAS* **391**, 935.
 Castro-Tirado, A. J., et al. (2008). *Nat* **455**, 506.
 Charlot, S. & Fall, S. M. (1993). *ApJ* **415**, 580.
 Chen, H.-W., Prochaska, J. X., Bloom, J. S., & Thompson, I. B. (2005). *ApJ* **634**, L25.
 Chen, H.-W., et al. (2007). *ApJL* **667**, L125.
 Christensen, L., Hjorth, J., & Gorosabel, J. (2004). *A&A* **425**, 913.
 Cobb, B. E. & Baylin, C. D. (2008). *ApJ* **677**, 1157.
 Costa, E., et al. (1997). *Nat* **387**, 783.
 Courty, S., Björnsson, G., & Gudmundsson, E. H. (2004). *MNRAS* **354**, 581.
 Courty, S., Björnsson, G., & Gudmundsson, E. H. (2007). *MNRAS* **376**, 1375.
 Crowther, P. (2007). *ARA&A* **45**, 177.
 D’Elia, V., et al. (2007). *A&A* **467**, 629.

- Djorgovski, G., et al. (2003). *Proc. SPIE* (Edited by Guhathakurta, Puragra) **4834**, 238.
- Elíasdóttir, Á., et al. (2009). *ApJ* **697**, 1725.
- Fenimore, E. E., et al. (1993). *Nature* **366**, 40.
- Fiore, F., et al. (2007). *A&A* **470**, 515.
- Foley, S., et al (2006). *A&A* **447**, 891.
- Fruchter, A. S., et al. (2006). *Nat* **441**, 463.
- Fynbo, J. P. U., et al. (2001). *A&A* **369**, 373.
- Fynbo, J. P. U., et al. (2002). *A&A* **388**, 425.
- Fynbo, J. P. U., et al. (2003a). *A&AL* **406**, L63.
- Fynbo, J. P. U., et al. (2003b). *A&A* **407**, 147.
- Fynbo, J. P. U., et al. (2005) *ApJ* **633**, 317.
- Fynbo, J. P. U., et al. (2006). *A&AL* **451**, L47.
- Fynbo, J. P. U., et al. (2008). *ApJ* **683**, 321.
- Fynbo, J. P. U., et al. (2009). *ApJS* **185**, 526.
- Galama, T. J., et al. (1998). *Nat* **395**, 670.
- Gehrels, N., et al. (2004). *ApJ* **611**, 1005.
- Greiner, J., et al. (2009). *ApJ* **693**, 1610.
- Groot, P., et al. (1998). *ApJL* **493**, L27.
- Hjorth, J., et al. (2012). *ApJ*, **756**, 187.
- Hogg, D. W. & Fruchter, A. S. (1999). *ApJ* **520**, 54.
- Hurley, K., et al. (1993). *A&AS* **97**, 39.
- Jakobsson, P., et al. (2004a). *ApJL* **617**, L21.
- Jakobsson, P., et al. (2004b). *A&A* **427**, 785.
- Jakobsson, P., et al. (2005a). *ApJ* **629**, 45.
- Jakobsson, P., et al. (2005b) *MNRAS* **362**, 245.
- Jakobsson, P., et al. (2006a). *A&A* **447**, 897.
- Jakobsson, P., et al. (2006b). *A&AL* **460**, L13.
- Jakobsson, P., et al. (2012). *ApJ* **752**, 62.
- Jaunsen, A. O., et al. (2008). *ApJ* **681**, 453.
- Kasliwal, M. M., et al. (2008). *ApJ* **678**, 1127.
- Kelly, P. L., Kirshner, R. P., & Pahre, M. (2007). *ApJ* **687**, 1201.
- Krühler, T., et al. (2008). *ApJ* **685**, 376.
- Krühler, T., et al. (2012). *ApJ* **758**, 46.
- Kulkarni, S., et al. (1998). *Nature* **393**, 35.
- Kurk, J., et al. (2000). *A&AL* **358**, 1.
- Larson, S. B. (1997). *ApJ* **491**, 86.
- Larsson, J., Levan, A. J., Davies, M. D., & Fruchter, A. S. (2007). *MNRAS* **376**, 1285.
- Lazzati, D., Covino, S., & Chisellini, G. (2002). *MNRAS* **330**, 583.
- Le Floc'h, E., et al. (2003). *A&AL* **400**, L499.
- Levan, A., et al. (2006). *ApJ* **647**, 471.
- Mao, S. & Mo, H. J. (1998). *ApJL* **339**, L1.
- Mas-Hesse, J. M., et al. (2003). *ApJ* **598**, 858.
- Metzger, M. R., et al. (1997). *Nature* **387**, 878.
- Michałowski, M., Hjorth, J., Castro-Cerón, J. M., & Watson, D. (2008). *ApJ* **672**, 817.
- Milvang-Jensen, B., et al. (2012). *ApJ* **756**, 25.
- Modjaz, M., et al. (2008). *AJ* **135**, 1136.
- Nagamine, K., Zhang, B., & Hernquist, L. (2008). *ApJ* **686**, L57.

- Natarajan, P., et al. (1997). *NewA* **2**, 471.
- Nuza, S. E., et al. (2007). *MNRAS* **375**, 665.
- Paczynski, B. (1998). *ApJL* **494**, L45.
- Pattel, M., et al. (2010) *A&AL* **512**, L3.
- Pedersen, K., et al. (2006). *ApJ* **636**, 381.
- Priddey, R. S., et al. (2006). *MNRAS* **369**, 1189.
- Prochaska, J. X., et al. (2003). *ApJL* **595**, L9.
- Prochaska, J. X., Chen, H.-W., Dessauges-Zavadsky, M., & Bloom, J. S. (2007). *ApJ* **666**, 267.
- Prochaska, J. X., et al. (2009). *ApJ* **691**, L27.
- Rol, E., et al. (2005). *ApJ* **624**, 868.
- Rol, E., et al. (2007). *ApJ* **669**, 1098.
- Ruiz-Velasco, A. E., et al. (2007). *ApJ* **669**, 1.
- Salvaterra, R. et al. (2010). *Nature* **461**, 1258.
- Sahu, K. S., et al. (1997). *Nature* **387**, 476.
- Savaglio, S. (2006). *NJP* **8**, 195.
- Schady, P. et al. (2010). *MNRAS* **401**, 2773.
- Silva, L., et al. (1998). *ApJ* **509**, 103.
- Soderberg, A., Djorgovski, S. G., Halpern, J. P., & Mirabal, N. (2004). *GCN* **2837**, 1.
- Starling, R.L.C., et al. (2005). *A&A* **442**, L21.
- Starling, R.L.C., et al. (2007). *ApJ* **661**, 787.
- Tanvir, N., et al. (2004). *MNRAS* **352**, 1073.
- Tanvir, N., et al. (2008). *MNRAS* **388**, 1743.
- Tanvir, N. et al. (2010). *Nature* **461**, 1254.
- van Paradijs, J., et al. (1997). *Nat* **386**, 686.
- van Paradijs, J., Kouveliotou, C., & Wijers, R. A. M. J. (2000). *ARAA* **38**, 379.
- Vreeswijk, P. M., et al. (2004). *A&A* **419**, 927.
- Vreeswijk, P. M., et al. (2007). *A&A* **468**, 83.
- Wijers, R. A. M. J., Bloom, J. S., Bagla, J. S., & Natarajan, P. (1998). *MNRAS Letters* **294**, L13.
- Wijnands, R. et al. (2009). *MNRAS* **393**, 126.
- Wolf, C. & Podsiadlowski, P. (2007). *MNRAS* **375**, 1049.
- Wolfe, A. M., Gawiser, E., & Prochaska, J. X. (2005). *ARA&A* **43**, 861.
- Woods, E. & Loeb, A. (1995). *ApJ* **453**, 583.

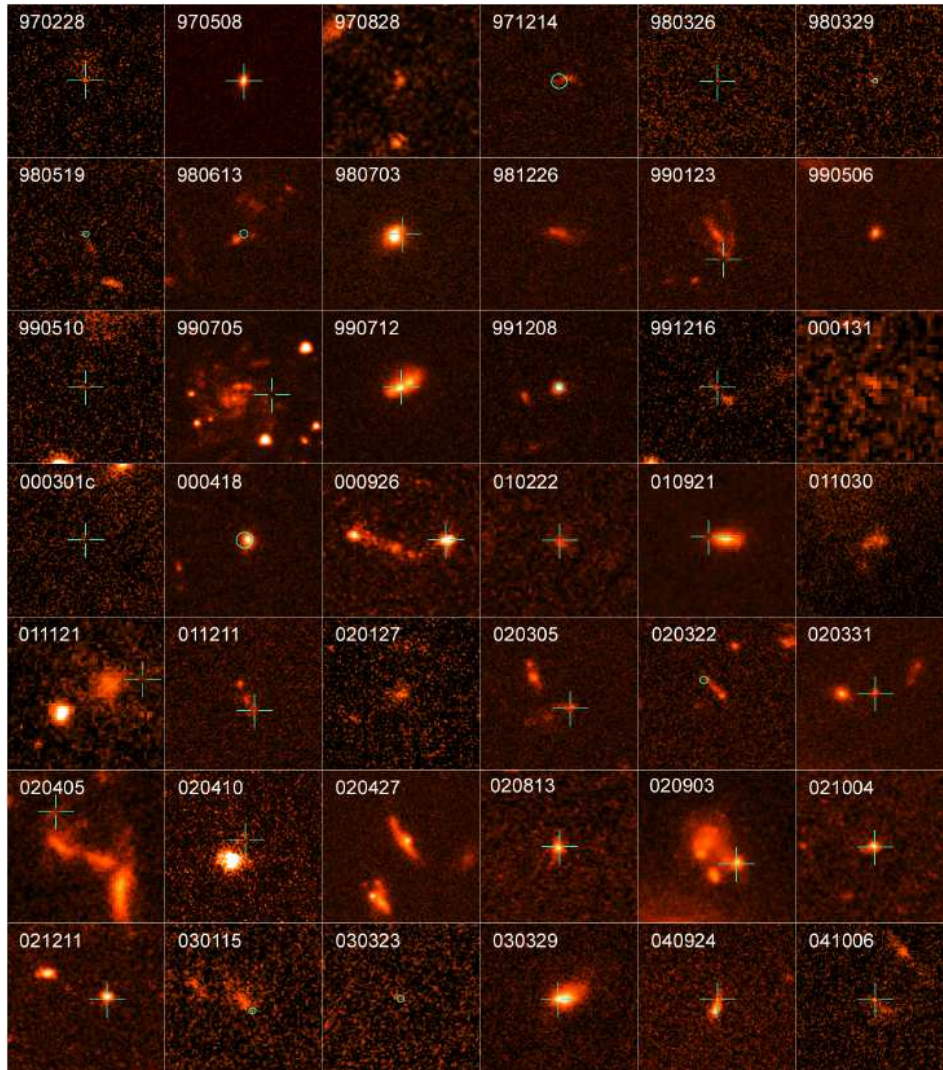


Fig. 13.4. A mosaic of GRB host galaxies imaged with *HST* (from Fruchter et al. 2006). Each individual image corresponds to a square region on the sky 3.75 arcsec on a side. These images were taken with the *HST*. In cases where the location of the GRB on the host is known to better than 0.15 arcsec, the position of the GRB is shown by a green mark. If the positional error is smaller than the point spread function of the image (0.07 arcsec for STIS and ACS, 0.13 arcsec for WFPC2) the position is marked by a cross-hair, otherwise the positional error is indicated by a circle. Due to the redshifts of the hosts, these images generally correspond to blue or ultra-violet images of the hosts in their rest frame, and thus detect light largely produced by the massive stars in the hosts.

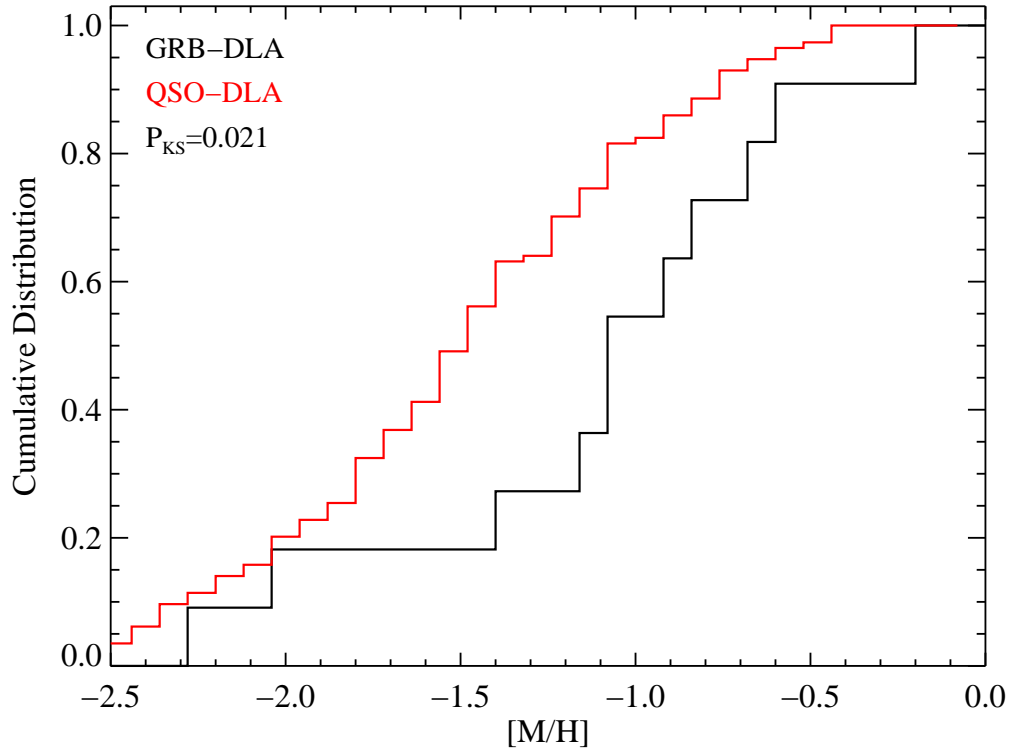


Fig. 13.5. The histograms show the cumulative distribution of QSO-DLA and GRB-DLA metallicities in the statistical samples compiled by Prochaska et al. (2003) and Prochaska et al. (2007). The GRB-DLA metallicities are systematically higher than the QSO-DLA metallicities. Based on a KS test, the probability that the two observed distributions are drawn from the same parent distribution is 2.1% (see also Fynbo et al. 2008 for a simple model of these two distributions).

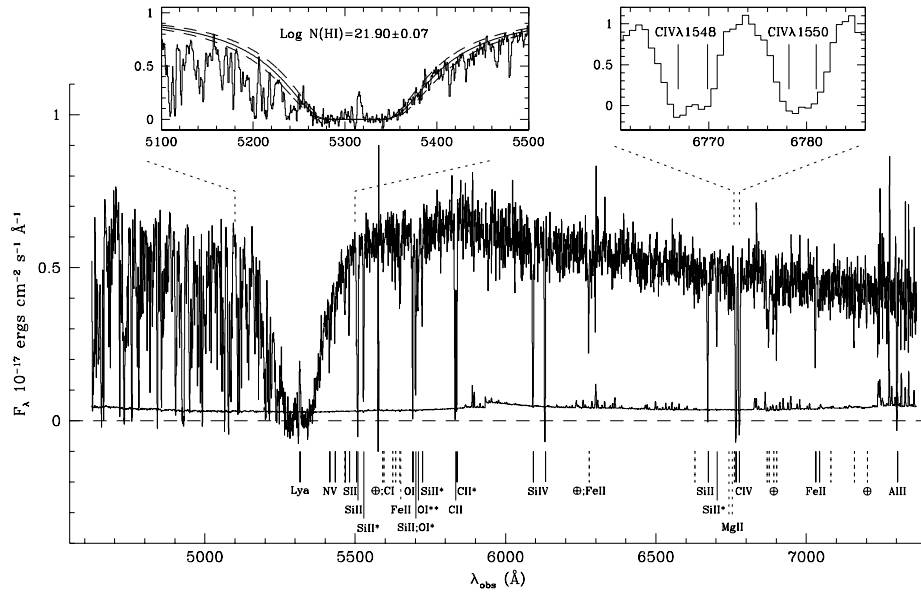


Fig. 13.6. The spectrum of the optical afterglow of GRB 030323 (from Vreeswijk et al. 2004). The insets show close-ups on the DLA (with Ly α in emission) and of the C IV doublet, showing the presence of at least two distinct components.

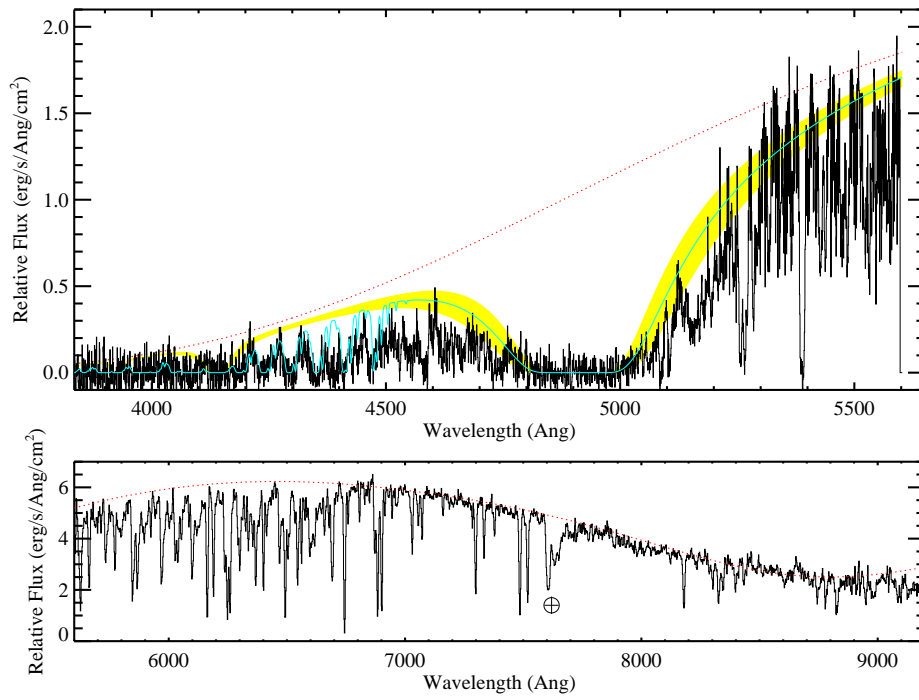


Fig. 13.7. The spectrum of the optical afterglow of GRB 080607 (from Prochaska et al. 2009).

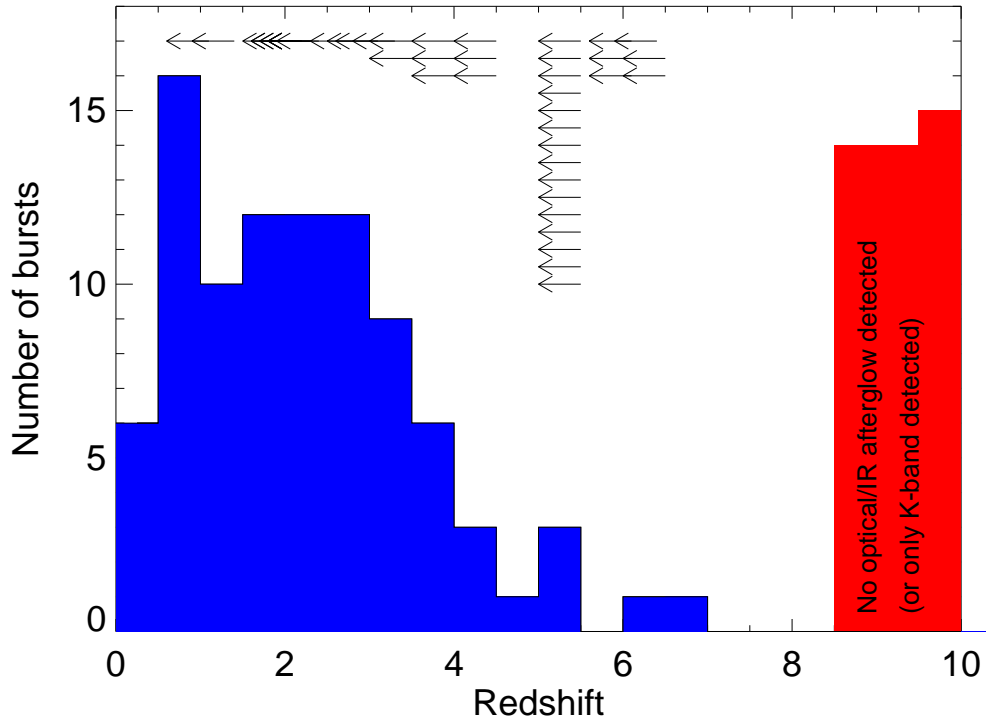


Fig. 13.8. Redshift distribution (up to March 2009) of *Swift* GRBs localized with the X-ray telescope and with low foreground extinction $A_V \leq 0.5$. Bursts for which only an upper limit on the redshift could be established so far are indicated by arrows. The histogram at the right indicates the bursts for which no optical/*J/H* afterglow was detected and hence no redshift constraint could be inferred (see Ruiz-Velasco et al. 2007 for a full discussion of an earlier version of this plot).

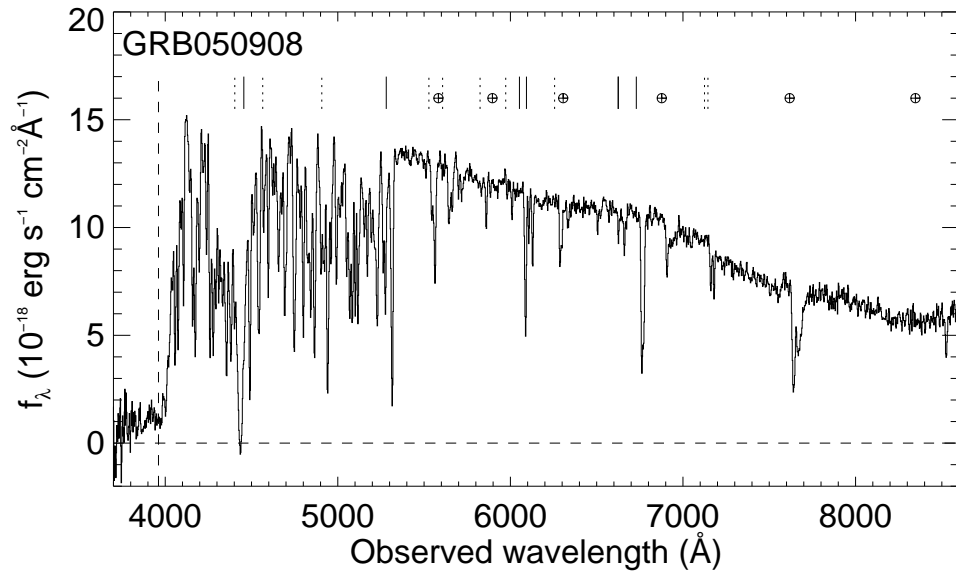


Fig. 13.9. The VLTFORS2 spectrum of the afterglow of GRB 050908 (Fynbo et al. 2009) Plotted is the flux-calibrated 1-dimensional spectrum against observed wavelength. The vertical dashed line shows the position of the Lyman limit at the redshift of the GRB ($z = 3.343$). As seen, there is clear excess flux blueward of the Lyman limit.

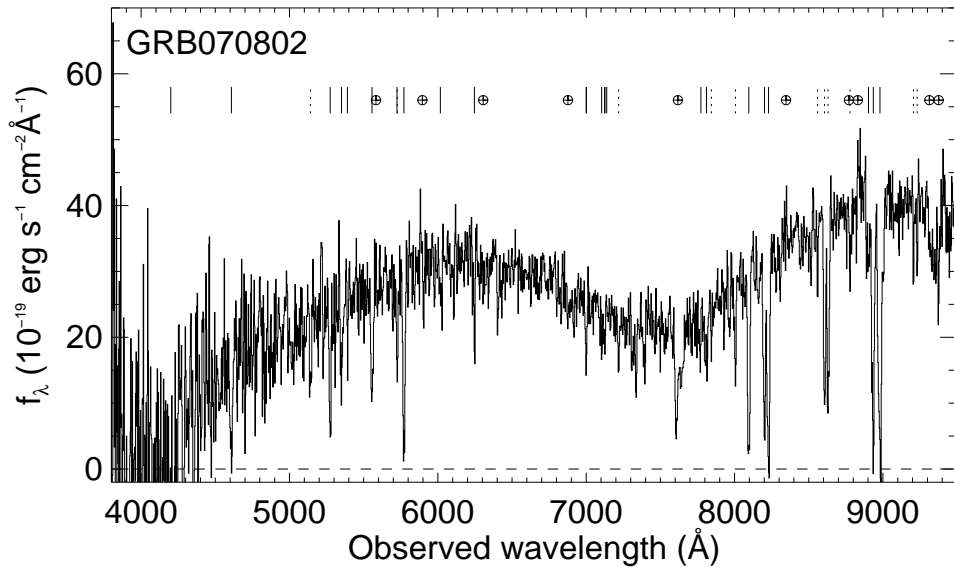


Fig. 13.10. The VLTFORS2 spectrum of the afterglow of GRB 070802 (Elíasdóttir et al. 2009). Plotted is the flux-calibrated spectrum against observed wavelength. Metal lines at the host redshift are marked with solid lines whereas the features from two intervening systems are marked with dotted lines. The broad depression centred around 7500 Å is caused by the 2175 Å extinction bump in the host system at $z_{\text{abs}} = 2.4549$.

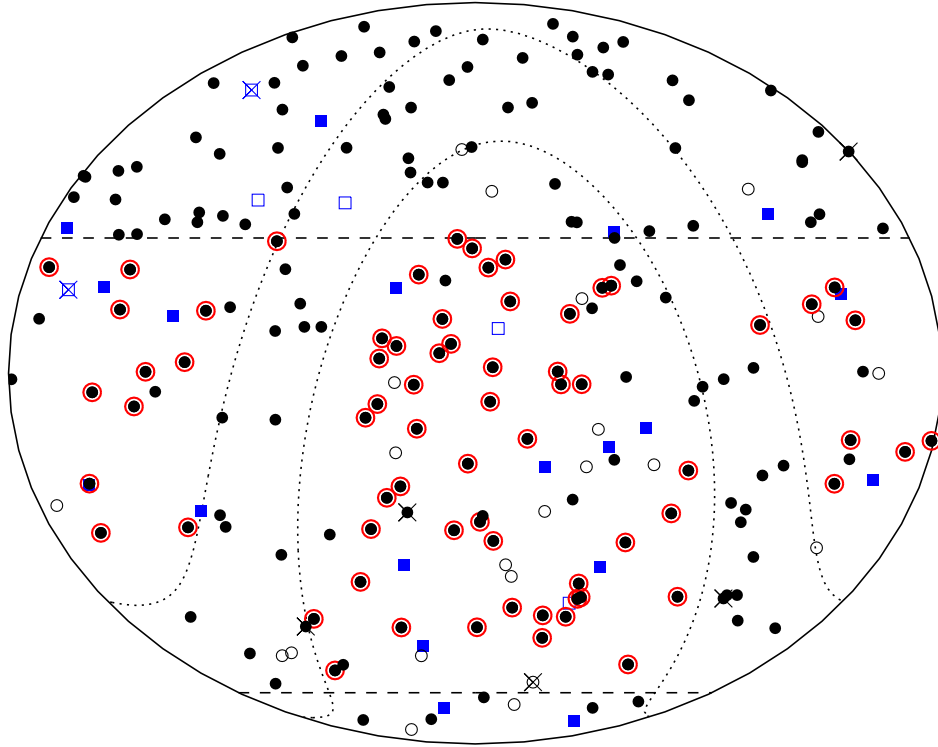


Fig. 13.11. All-sky map (Mollweide projection) of the 238 *Swift* GRBs occurred between 2005 March and 2007 August. Empty circles: GRBs with no *Swift*/XRT detection. Filled circles: GRBs with *Swift*/XRT detection. Filled, encircled circles: GRBs obeying all selection criteria of the Hjorth et al. (2010) sample. Squares: GRBs classified as short. Crosses: nontriggered GRBs. Overplotted are the declination cuts (-70 and $+27^\circ$, dashed lines) and the region with Galactic latitude $|b| > 20^\circ$ (dotted curves), which roughly corresponds to the sample selection criterion $A_V < 0.5$ mag.

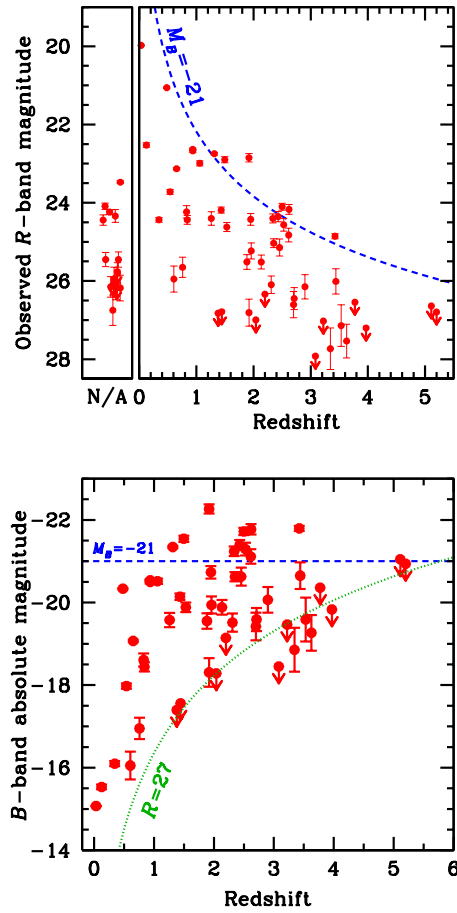


Fig. 13.12. Top: observed R -band magnitudes of the hosts in the Hjorth et al. (2012) sample as a function of redshift. The left panel shows objects with unknown redshift (the x -axis value is arbitrary). The dashed line shows the magnitude of an L^* galaxy ($M_B = -21$) as a function of redshift. Bottom: absolute luminosity of hosts as a function of redshift. The dashed line shows the level of L^* , while the dotted curve indicates the effective survey limit ($R \sim 27$).

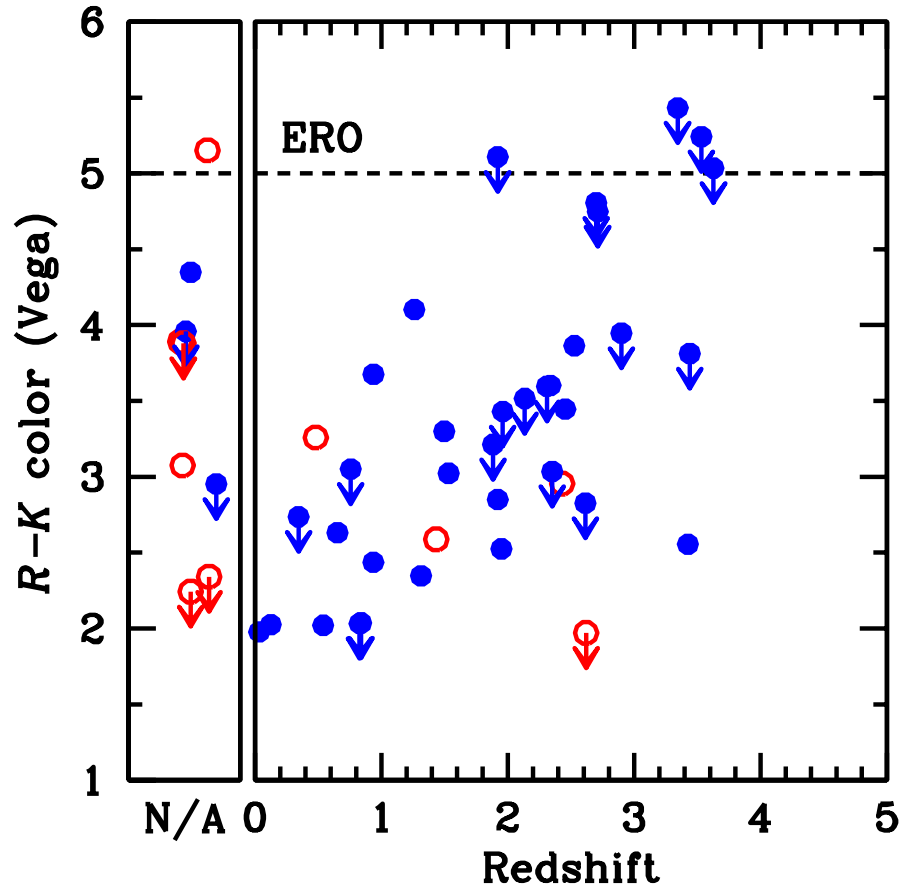


Fig. 13.13. $R - K$ colour of the hosts in the Hjorth et al. (2012) sample as a function of z . Filled symbols are for GRBs with detected optical afterglows and open symbols for GRBs with no detected optical afterglow. Only the galaxies with optical detections are shown. The left panel shows systems with no known redshift (the x -axis value is arbitrary). The horizontal line marks the boundary of extremely red objects (EROs; $R - K > 5$).

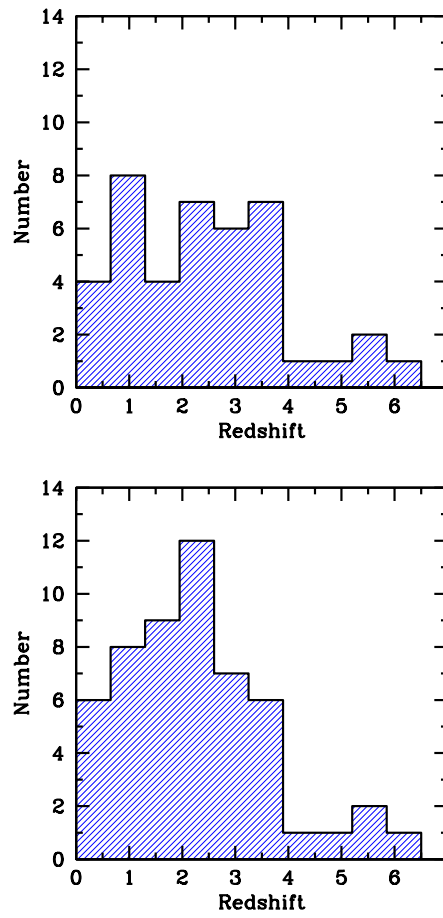


Fig. 13.14. Redshift distribution of GRBs in the Hjorth et al. (2012) sample. Top panel: redshifts taken from the literature. Bottom panel: including the results from host spectroscopy in the program.

